Agricultural and Forest Meteorology 342 (2023) 109734

Contents lists available at ScienceDirect

Agricultural and Forest Meteorology

journal homepage: www.elsevier.com/locate/agrformet

Spring photosynthetic phenology of Chinese vegetation in response to climate change and its impact on net primary productivity

Yingying Xue [a,b], Xiaoyong Bai [a,c,*], Cuiwei Zhao [b], Qiu Tan [b], Yangbing Li [b], Guangjie Luo [d], Luhua Wu [a], Fei Chen [a,e], Chaojun Li [a], Chen Ran [a,b], Sirui Zhang [a,b], Min Liu [a,b], Suhua Gong [a], Lian Xiong [a,b], Fengjiao Song [a], Chaochao Du [a,b], Biqin Xiao [a,b], Zilin Li [a,b], Mingkang Long [a]

[a] *State Key Laboratory of Environmental Geochemistry, Institute of Geochemistry, Chinese Academy of Sciences, 99 Lincheng West Road, Guiyang, Guizhou Province 550081, China*
[b] *School of Geography and Environmental Sciences, Guizhou Normal University, Guiyang, Guizhou Province 550025, China*
[c] *CAS Center for Excellence in Quaternary Science and Global Change, Xi'an, 710061, China*
[d] *Guizhou Provincial Key Laboratory of Geographic State Monitoring of Watershed, Guizhou Education University, Guiyang 550018, China*
[e] *College of resources and environmental engineering, Guizhou University, Guiyang 550025, China*

ARTICLE INFO

Keywords:
Photosynthesis
Phenology
Climate change
Net primary productivity
Solar-induced chlorophyll fluorescence
China

ABSTRACT

In the context of global warming, the advancement of spring phenology in northern and temperate regions due to increased temperatures has been widely reported. Early and delayed start of the photosynthetic period (SOP) directly affects the vegetation net primary productivity (NPP). However, the interrelationship between climate change, the SOP, and the NPP is unclear. In this paper, we use the dynamics of decadal daily solar-induced chlorophyll fluorescence data to calculate the response of Chinese vegetation photosynthetic phenology to climate change and its impact on the NPP over the last 20 years. The results found that over the last 20 years, the average SOP in China was on the 123rd day of the year, and the SOP has advanced at an average rate of 4.3 d (10 a)$^{-1}$, with a faster trend of SOP advancement in highland and high-altitude areas. 64% of SOP in China is controlled by temperature; 36% of the SOP in China is controlled by precipitation, and the relative importance of temperature and precipitation was reversed as the precipitation gradient decreased, with SOP dominated by temperature when pre-season precipitation ≧300 mm, and SOP dominated by precipitation when pre-season precipitation ≦300 mm. Finally, we find that climate change indirectly increases vegetation NPP by advancing SOP. Our study emphasizes the importance of precipitation on phenology. It provides a scientific basis for understanding and predicting the response of spring photosynthetic phenology to climate change and the contribution of spring phenology to carbon estimation in terrestrial ecosystems.

1. Introduction

Plant phenology, the cyclical growth and development of vegetation in the natural environment, is considered to be one of the most sensitive indicators of climate change, and changes in phenology have a strong impact on the carbon cycle, water cycle and energy exchange in terrestrial ecosystems and the feedback to the climate (Piao et al., 2007; Shen, 2022; Wang, 2022a). Significant increases in vegetation primary productivity due to earlier spring photosynthesis as a result of climate change have been widely reported (Keeling et al., 1996; Piao et al., 2019), especially in China (Yao et al., 2018). Therefore it is crucial to quantify the contribution of climate change to the onset of photosynthetic phenology and its impact on net primary productivity.

Previous studies on the response of phenology to climate change have utilized many methods, such as traditional ground-based observations (Aono and Kazui, 2008), which can accurately record changes in phenological events in specific locations and species. Operational experiments are also very useful methods, and two broad climate warming experiments, passive and active warming, have been used in phenological studies (Aronson and McNulty, 2009). Both methods suggest that warming causes an earlier spring phenology. In addition, phenological modeling is a common way to understand phenological responses to climate change (Hunter and Lechowicz, 1992). In recent years, phenological responses to climate based on remote sensing observations have

* Corresponding author.
E-mail address: baixiaoyong@vip.skleg.cn (X. Bai).

https://doi.org/10.1016/j.agrformet.2023.109734
Received 9 April 2023; Received in revised form 20 September 2023; Accepted 24 September 2023
Available online 27 September 2023
0168-1923/

been used as the most common means (Liu et al., 2016; Piao et al., 2017b; Smith et al., 2018; Tan et al., 2023; Zeng et al., 2020b), compared with other methods, its application greatly improves the observation range and accuracy of the phenology. Previous studies on large-scale spring phenology have focused on temperate and boreal regions (Parmesan, 2007; Ren et al., 2022; Ren and Peichl, 2021), particularly by examining changes in vegetation indices related to greenness in time series, such as the leaf area index (LAI), normalized difference vegetation index (NDVI), and enhanced vegetation index (EVI), etc. (Paulina et al., 2017; Piao et al., 2006; Wang, 2014a). This is because in boreal and temperate deciduous species and grassland, the seasonal dynamics of leaf greening and yellowing are apparent, so their return and yellowing periods are easily detected (Fu, 2022a; Piao, 2019; Zeng et al., 2020a).

Previous studies on boreal and temperate forests and grassland have generally concluded that climate warming has advanced the spring phenology of vegetation (Gill et al., 2015; Ma et al., 2022a; Piao et al., 2006; Ren et al., 2022; Steltzer and Post, 2009; Zhang et al., 2013). Other studies have shown that in addition to climate warming the winter temperature (Murray et al., 1989; Wang et al., 2015), average pre-season temperature (Piao et al., 2006), daily maximum and minimum temperatures (Shen et al., 2018), diurnal temperature difference (Shen et al., 2018), accumulated precipitation (Ren et al., 2022; Shen et al., 2011a), photoperiod (Richardson et al., 2013) snow melt (Chen et al., 2015) and other factors are also key factors affecting the phenology of northern and temperate forests and grasslands. Recent studies have shown that the sensitivity of the SOP to temperature has gradually decreased (Wang et al., 2014b), and precipitation plays an increasingly significant role in the initial stage of photosynthesis (Ma et al., 2023; Shen et al., 2015b). For example, Li et al.(2021b) found that the importance of the SOP precipitation in subtropical forests in China increases with decreasing latitude. Li et al. (2023a) found that insufficient precipitation will limit the response of the SOP to warming, and precipitation determines the light-heat use efficiency of vegetation to a certain extent, thus affecting the spring phenology. However, most previous studies have been based on the assumption that temperature plays a dominant role (Chen et al., 2018; Dai et al., 2021; Piao et al., 2017b) and have ignored the effect of precipitation on the SOP. Under the background of future warming and drying of the conditions climate, it is necessary to study the key drivers of the SOP under different precipitation gradients.

In addition, it has been suggested that the early spring phenology of vegetation is one of the main factors in the increase in carbon uptake (Gu et al., 2022; Hu et al., 2010). Each day in advance of the SOP leads to an increase of 45 kg of net carbon uptake per hectare of forest (Keenan et al., 2014). Others believe that the advance of the spring phenology will increase evapotranspiration and consume available soil water, resulting in summer drought, but they negated the positive role of spring phenology in carbon absorption (Buermann et al., 2013; Lian et al., 2020). Therefore, these complex coupling effects therefore make the role of the SOP in terrestrial ecosystem productivity unclear, and exploring the climate-SOP-NPP relationship is critical to improving our understanding of the global water and carbon cycles under global climate change conditions.

Previous studies have calculated the SOP by detecting changes in the vegetation greenness (Paulina et al., 2017), and canopy greenness satellite products have been widely used as indicators of vegetation photosynthesis and productivity(Forkel et al., 2016). However, recent studies have shown that the greenness is decoupled from the productivity in dry years and in drought-prone areas (Hu et al., 2022), that is, greenness of vegetation does not coincide with its photosynthesis. In addition, the dynamics of the greenness are not obvious in evergreen vegetation areas, where the physiological phenology (i.e., photosynthesis-based phenology) undergoes seasonal changes while the upper canopy (i.e., leaf greenness) remains stable (Li et al., 2021a), making it difficult to detect the phenology using the commonly used vegetation indices of greenness (Schwartz, 2003). Therefore, it is inappropriate to use canopy greenness satellite products to calculate the nationwide SOP. Recent satellite inversion-based solar-induced chlorophyll fluorescence (SIF) offers a new approach to SOP calculations (Li et al., 2018a; Piao et al., 2019). The SIF is the re-emission of a small fraction of the absorbed radiation, and in general, 1% of the solar energy captured by plants is re-emitted by chlorophyll as fluorescence with two peaks in the red (around 690 nm) and near-infrared (around 740 nm) bands that can be detected from space by current high spectral resolution sensors (Zhang et al., 2014a). SIF is directly related to photosynthesis through a complex energy dissipation mechanism, can be used as a proxy for photosynthesis (Chen et al., 2021), and is less affected by cloud, snow, and ice cover (Gentine and Alemohammad, 2018). Thus, satellite-based SIF observations provide an alternative physiologically based view of the contribution of vegetation function to the structural and greenness information provided by traditional reflectance indices, and can be used as an alternative toll for data estimation of vegetation photosynthetic phenology tool (Jeong et al., 2017; Joiner et al., 2014), that is more directly related to the carbon cycle and the effects of climate change (Chen et al., 2022b).

In this study, we investigated the temporal changes in the onset of photosynthesis in China over the last 20 years based on the spatially contiguous solar-induced fluorescence (CSIF) dataset from the global orbiting carbon observatory (OCO-2), and we studied the relationship between the SOP and climate and its contribution to productivity in China using partial correlation analysis and structural equation modeling.. The aims of this study were (1) to assess the magnitude, spatial patterns and dynamic trends of annual SOP changes in China over 20 years; (2) to illustrate the response of the SOP to climate change in China; and (3) to reveal the impact of SOP on productivity. We used the SIF data to calculate an SOP based on vegetation physiological dynamics rather than the traditional greenness-based phenology, which is directly related to photosynthesis. We studied the main driving factors of SOP under different precipitation gradients, which has important reference significance for predicting the response of the SOP to climate under the background of future warming and drying of climate conditions. Finally, we studied the climate-SOP-NPP interaction across the country. The results of this study are of great significance for understanding and predicting the response of the initial photosynthetic phenology period to climate change and its impact on the productivity of terrestrial ecosystems in the future and provide a scientific basis for the estimation of the carbon sink in terrestrial ecosystems. Furthermore, we hypothesize that (1) Climate change drives earlier trends in SOP (2) Climate change has a direct effect on SOP and then an indirect effect on NPP through SOP.

2. Dadaset and methods

2.1. Study area

The study focuses only on mainland China, a vast country that spans tropical, subtropical, warm and temperate regions from south to north; From east to west, it includes humid, semi-humid, semi-arid, arid and ultra-arid, We have divided the study into four main regions (As shown in Fig. 1): (1)Northern Region (NR), The average annual temperature ranges from −4 °C to 14 °C, and the total annual precipitation ranges from 200 mm to 1000 mm in Northwest China (Yang et al., 2017). (2) The Northwest Region (NWR), the average annual temperature ranges from 0 °C to 8 °C, and the average annual precipitation is less than 600 mm (Yang et al., 2017). (3) The Qinghai-Tibet Plateau Region (QTR) is known as the third pole of the world and has an average altitude of nearly 4000 m. The average annual temperature ranges from −5 °C to 12 °C and the precipitation ranges from 800 mm to 200 mm (Shen et al., 2011b). (4) Southern Region (SR), the average annual temperature is 14 °Cto 22 °C, and the total annual precipitation is 1000mm-2000 mm (Wang et al., 2015b). The temperature gradient in China is larger from

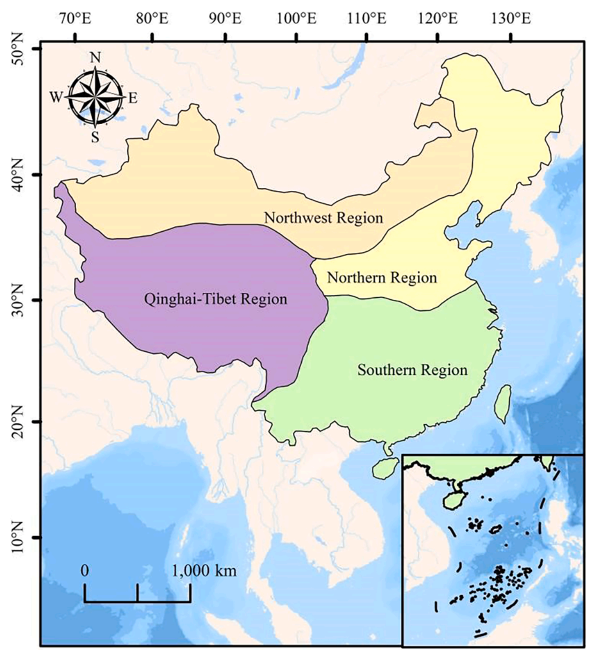

Fig. 1. Location map of the study area.

south to north, and the precipitation gradient from south to north is larger. Therefore, China is ideal for examining the response of phenology to climate change at a regional level (Li and Zha, 2019).

2.2. Datasets

2.2.1. daylight-induced chlorophyll fluorescence

As a proxy for photosynthesis, we used daylight-induced chlorophyll fluorescence (SIF) data to calculate the SOP. Existing SIF data have short time span and low resolution, and these shortcomings limit the application of SIF (Zhang et al., 2018). Recently, Zhang et al. combined the SIF retrieved from the Orbiting Carbon Observatory (OCO-2) satellite and the surface reflectance from the Moderate Resolution Imaging Spectroradiometer (MODIS) on board the Terra and Aqua satellites, and applied machine learning and neural network algorithms to generate a global continuous CSIF product, which supplements the insufficient temporal and spatial resolution of the OCO-2 data, which is comparable to that of the OCO-2 and the Global Ozone Monitoring Experiment-2 (GOME-2) daily SIF (Zhang et al., 2018). We therefore chose to use CSIF data, which has been published in the National Third Pole Environment Data Center (https://data.tpdc.ac.cn/en/), with a temporal resolution of 4 days and a spatial resolution of 0.05°

2.2.2. Climate data set

We used temperature and precipitation data from 2001 to 2020, sourced from the National Earth System Science Data centre (https://www.geodata.cn/), The temporal resolution is month and the spatial resolution is 0.0083333°(about 1 km). Based on global 0.5° climate data released by CRU and global high-resolution climate data released by WorldClim, the data were generated in China by Delta spatial downscaling scheme. It was verified with data from 496 independent meteorological observation points, and the verification results were credible, which has been widely applied to ecology, geoscience and other fields (Li et al., 2022, 2023b; Peng et al., 2021; Yu et al., 2022).

2.2.3. NPP data

MODIS Terra from 2001 to 2020, provided by the National Aeronautics and Space Administration (NASA), was used for this study NPP data (MOD17A3HGF) (https://search.earthdata.nasa.gov/search), temporal resolution for years, the spatial resolution of 0.0044915764° (500 m). We use the professional processing TOOL MRT TOOL provided by MODIS website for projection conversion, stitching, cropping and other work.

2.2.4. land use and land cover change data (LUCC)

Since the cultivated land phenology is greatly influenced by human subjectivity, in order to ensure the accuracy of the study, cultivated land types were excluded in this study according to the LUCC data provided by Data Center for Resources and Environmental Sciences (https://www.resdc.cn/).

Finally, all the data were resamped to the same spatial resolution (0.05°) as the CSIF data to facilitate our research. The resampling method we adopted was bilinear interpolation, which had high interpolation accuracy and moderate computation, and was suitable for continuous data. This interpolation method could generate smoother surfaces.

2.3. Methods

2.3.1. SOP methods

We carried out a polynomial fit analysis between the 4-day CSIF time series data for the whole study area from January to December and the corresponding dates to obtain a smooth seasonal curve of the annual CSIF time series for each pixel, removing anomalies due to the influence of cloudiness, atmosphere, etc. (Piao et al., 2006; Zhang et al., 2013).

$$SIF = a + a_1x^1 + a_2x^2 + +a_3x^3 + \ldots + a_nx^n, n = 6 \tag{1}$$

Here x corresponds to a day of the year in the SIF and a is a coefficient. The vegetation growth curve was then fitted with a hybrid segmented logistic function (Zhang et al., 2022c) to determine SOP timing and was more suitable for fitting vegetation growth at high latitudes than other fitting methods, and we used spring photosynthetic phenology as the corresponding CSIF value to reach 20% of the seasonal amplitude, respectively, a threshold that follows previous phenology studies (Buyantuyev and Wu, 2012; Cong et al., 2013b; Qiu et al., 2020; Zhou et al., 2016), and this threshold was also used in the VIIRS land surface phenology product. The formula is as follows:

$$f(t) = a_1 + \frac{a_2}{1 + e^{-\theta_1(t-\beta_1)}} - \frac{a_3}{1 + e^{-\theta_2(t-\beta_2)}} \tag{2}$$

where parameters a1, a2 and a3 represent the minimum values of the seasonal cycle, the amplitude of the seasonal cycle before and after, θ1 and θ2 are coefficients that determine the rate of vegetation growth and senescence, and β1 and β2 are fit parameters.

2.3.2. Theil-Sen Median analysis and Mann-Kendall mutation test

The Theil-Sen Median is a robust, non-parametric statistical method of trend calculation. This method is computationally efficient, independent of outliers and is often used in trend analysis of long time series data (Li et al., 2018b):

$$Sen = Median\left(\frac{x_i - x_j}{i - j}\right) \tag{3}$$

where x, y denote SOP values in year i and j respectively, and median is the median of the time series, usually used in conjunction with the Mann-Kendall test to further determine the significance of the trend, which has the advantage of calculating samples that do not have to follow a specific regular distribution (Kendall, 1938; Ran et al., 2023). Results vary significantly at the $p < 0.05$ level.

2.3.3. Partial correlation analysis

In order to further identify the dominant climatic factors in SOP, a bias correlation analysis was performed between SOP and 'pre-seasonal' climate for each of the 20 years of the year, with pre-season defined as the period with the largest bias correlation coefficient between SOP and climatic variables (Chen et al., 2022a; Li et al., 2021a; Meng et al., 2021; Piao et al., 2007; Xiao et al., 2023), where precipitation is cumulative precipitation and temperature is average temperature.

$$R_{x_1 y} = \frac{R_{yx_1} - R_{yx_2} R_{x_1 x_2}}{\sqrt{\left(1 - R_{yx_2}^2\right)\left(1 - R_{x_1 x_2}^2\right)}} \quad (4)$$

$R_{x_1 y}$is the partial correlation coefficient of the x1 factor, R_{yx_1} R_{yx_2} $R_{x_1 x_2}$are the simple correlation coefficients between x1 and the dependent variable y, x2 and y, x1 and x2 respectively.

2.3.4. Structural equation model

We used AMOS 26 software to construct the Structural equation model (SEM), a multivariate statistical method based on the covariance matrix, which is a multivariate analytical equation that includes statistical methods such as factor analysis and path analysis. Based on theoretical research and empirically developed conceptual models, SEM can capture direct, indirect and combined effects between variables (Stone, 2021). The method has been applied to the fields of ecology and climatology (Hao et al., 2020; Weterings et al., 2018; Ye et al., 2022). The interrelationship between temperature, precipitation, SOP and NPP is complex. In order to reveal the impact of SOP advancement on NPP, we used SEM model to evaluate the direct and indirect relationships between climate factors, NPP and SOP.

In this study, the maximum likelihood method in SEM modeling was used to estimate the path coefficients and each parameter. All the models have chi-square degrees of freedom less than 3 and root mean square error RMSEA less than 0.05.The model fit is good.

3. Results

3.1. Spatial and temporal distribution pattern of SOP in China

The average SOP for vegetation in China during the last 20 years was on the 123rd day of the year (Fig. 2a), and the vegetation photosynthetic phenology has obvious spatial specificity in different regions, exhibiting a gradual delay from low to high latitudes (Fig. 3a). On average, the SOP in the SR occurs earliest, concentrated in 70–100 days, and the SOP in the QTR occurs latest, concentrated in 130–160 days. In addition, the SOPs in the NWR and NR are concentrated in the ranges of 110–140 days and 90–120 days respectively (Fig. 2a). In terms of the inter-annual trends, the average SOP in China advanced at a rate of 0.43 days per year. The interannual trend was fastest (0.48 days per year) in the QTR and slowest (0.25 days per year) in the NWR, and it advanced at ranges of 0.44 days per year and 0.45 days per year in the NR and SR, respectively (Fig. 1b). The greatest trend fluctuations occurred in the mid-latitude region (Fig. 3b).

In terms of the spatial trends, the SOP overwhelmingly advanced in the last 20 years with a trend of 0–0.5 days/a (Fig. 2c).According to the Mann-Kendall (M-K) test, the spatially advanced SOP trend accounted for 71% of the elements, of which 25% were significantly advanced, mainly in the northern Tibetan Plateau, the Yunnan-Guizhou Plateau, the western Loess Plateau, the southern hills and the Greater Khingan Mountains region (Fig. 2d). The SOP exhibite a delayed trend in 20% of the elephant elements, mainly in the southern Qinghai-Tibet Plateau and northwestern Inner Mongolia, with significant delays in only 3% of the areas (Fig. 2d). We found that the SOP tend to advance more rapidly in highland and high-altitude areas. In general, the SOP in China exhibited show an overall trend of non-significant advancement over a large area.

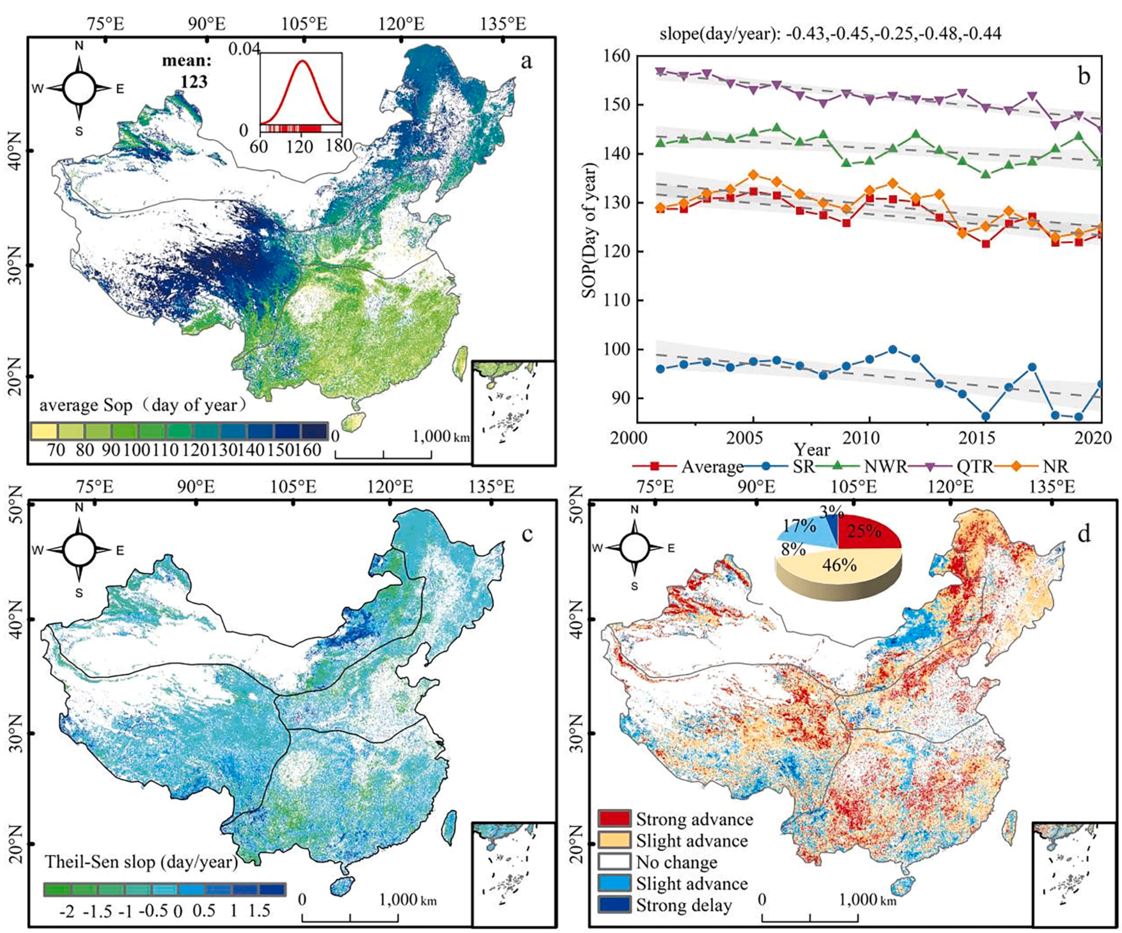

Fig. 2. Spatial distribution of multi-year average SOP (a) Interannual trend (b) Theil-sen Slop trend of SOP in the last 20 years (c) Theil-sen Slop after M-K test.

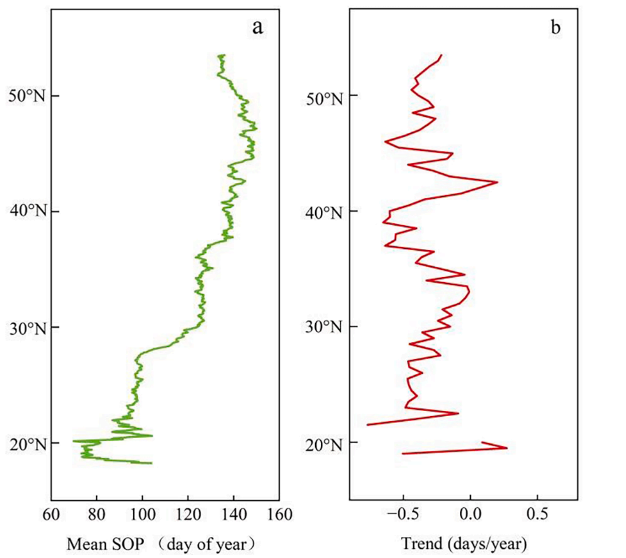

Fig. 3. Latitudinal distribution of the average SOP over the last 20 years (a) Latitudinal distribution of trends (b).

3.2. Climate determinants of SOP

The bias correlation coefficients between the SOP and the pre-season temperature and precipitation are shown in Figs. 4a–b. It can be see that the pre-season temperature was often negatively correlated with the SOP in approximately 76% of the total pixels, (with 16.1% being significantly negatively correlated ($p < 0.05$). This mainly occurred in the central QTR, northeastern SR and NR areas (Fig. 4a). The positive correlation between the pre-season temperature and the SOP accounted for the remaining 24% of the pixels (of which 0.9% were significantly positively correlated), mostly sporadically in the southern part of QTR and the north-western part of the NWR (Fig. 4a). In contrast, the positive correlation coefficient of the bias between the precipitation and the SOP was about 46% (with 3.36% exhibiting a significant positive correlation), mainly in the eastern coastal zone of the SR and the northeastern part of the study area. The negative correlation coefficient between the precipitation and SOP was approximately 53.8% (with 5.53% exhibiting a significant negative correlation), mainly in the central QTR and western SR.

The spatial distributions of the relative importance of the temperature and precipitation in each pixel are shown in Fig. 4c (the quadrant defined as the maximum value of the bias correlation coefficience between the SOP and precipitation and temperature), and the proportion of the quadrants for the main controls of the temperature and precipitation at different pre-season precipitation gradients is shown in Fig. 4d. Temperature determined 53% of the quadrates across the study area, while precipitation determined 47% (Fig. 4c). Interestingly, the determinant of the elephant element changed from temperature to precipitation as the precipitation gradient decreased. Using the average pre-season precipitation of 300 mm as the boundary, the SOP was dominated by temperature control when the pre-season precipitation was ≧ 300 mm. When the pre-season precipitation was ≦ 300 mm, the SOP was

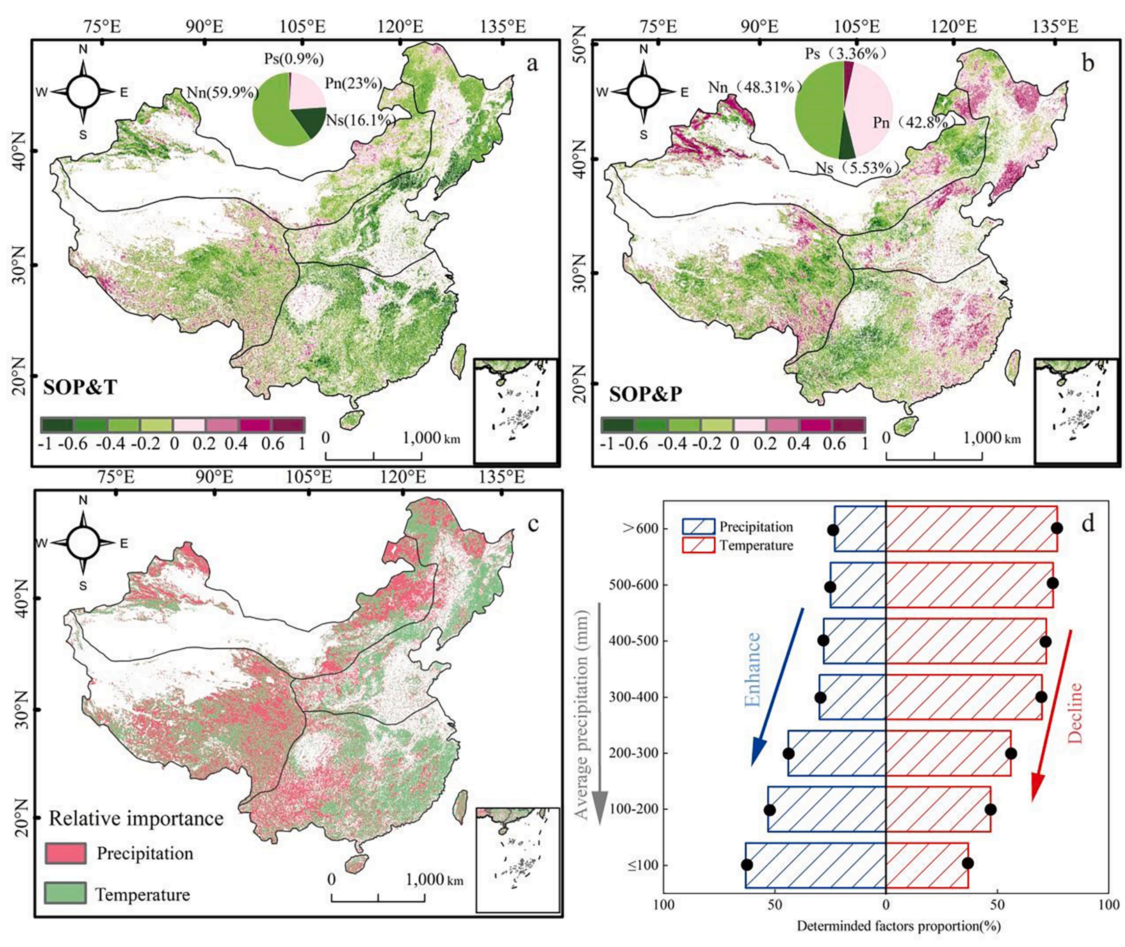

Fig. 4. (a-b) Spatial patterns of bias correlation coefficients between temperature and precipitation and SOP, with inserted pie charts indicating Ps (positive significant), Pn (positive non-significant), Ns (negative significant), Nn (negative non-significant), spatial distribution of the main climate controls on SOP in the study area (c), and the share of the main controls in the different precipitation conditions (d).

dominated by precipitation control, i.e., temperature was the main determinant of the SOP in areas with sufficient precipitation, while precipitation was the main determinant of the SOP in areas with pre-season water deficit.

3.3. Effect of SOP advancement on net primary productivity of vegetation as indicated by SEMs

In Fig. 5, the structural equation model (SEM) shows that there were complex interactions between the temperature, precipitation, SOP, and NPP in the four regions. In addition to the significant negative direct effect of the SOP on the NPP in the NWR, the temperature and precipitation indirectly affected (negatively affected) NPP in the NWR by influencing the SOP, and the indirect effect of temperature (flux coefficient: 0.603) on the NPP was greater than that of precipitation (flux coefficient: 0.308). The effect of the SOP on NPP was also significant in the NR area. Although temperature and precipitation still had indirect effects on the SOP, there effects were not significant. In the QTR area, the effect of the SOP on the NPP was not significant, but both temperature and precipitation significantly and negatively affected the NPP indirectly, and the indirect effect of temperature (flux coefficient: 0.5) was greater than that of precipitation (flux coefficient: 0.407). In the SR area, the NPP was significantly directly influenced by the temperature and SOP. The temperature significantly influenced the NPP by indirectly influencing the SOP, and precipitation did not have a significant effect on the NPP in the SR area.

In summary, the NPP was negatively and indirectly influenced by the temperature and precipitation in all four regions, and the temperature most significantly affected the NPP indirectly by influencing the SOP. The hypothesis that climate change has advanced the SOP and thus increased the vegetation NPP is supported.

4. Discussion

4.1. Spatial and temporal distributions pattern of SOP

We compared the SOP calculated in this study with the results of previous studies to further confirm the reliability of our results The spatial pattern identified in this study is similar to that reported in previous studies, i.e., a gradual delay from low latitude to high latitude and a faster advancement of the SOP at high altitudes (Cong et al., 2013b; Jiao et al., 2020; Luo and Yu, 2017; Ma and Zhou, 2012; Wang et al., 2022b). However, the trends are different. For example, based on EVI data, Jiao et al. (2020) calculated that the SOP advanced by 2.88 days per decade from 1981 to 2016. Based on four methods, namely, species observation, meta-analysis, remote sensing influence, and phenological modeling, Ma et al. (2012) concluded that the SOP in China has advanced by 2.88 days every decade. These results are less than our results (4.3 days earlier per decade), which may be because we calculated the phenology based on photosynthesis, while previous studies were based on the phenology of the greenness. In addition, differences in the research periods will lead to some deviations. In addition, comparative studies have also shown that the SOP calculated based on the SIF is earlier than that based on the NDVI and EVI (Wang et al., 2022c). In addition, based on meta-analysis, Zhang et al. (2022a) concluded that the SOP advanced at a rate of 0.23 ± 0.47 days/a over the last 40 years and our results are within their range. In addition, Li et al. (2021b) used SIF data and various methods (Gaussian-midpoint method, piecevise logistic method, HANTS-maximum method, and spline-midpoint method) to calculate the SOPs of 91 ± 9 days for Chinese subtropical mixed evergreen-deciduous forests, 87 ± 7 days for Central Asian evergreen forests, and 72 ± 8 days for southern monsoon evergreen forests, which are similar to our findings. Therefore, we consider our findings to be credible.

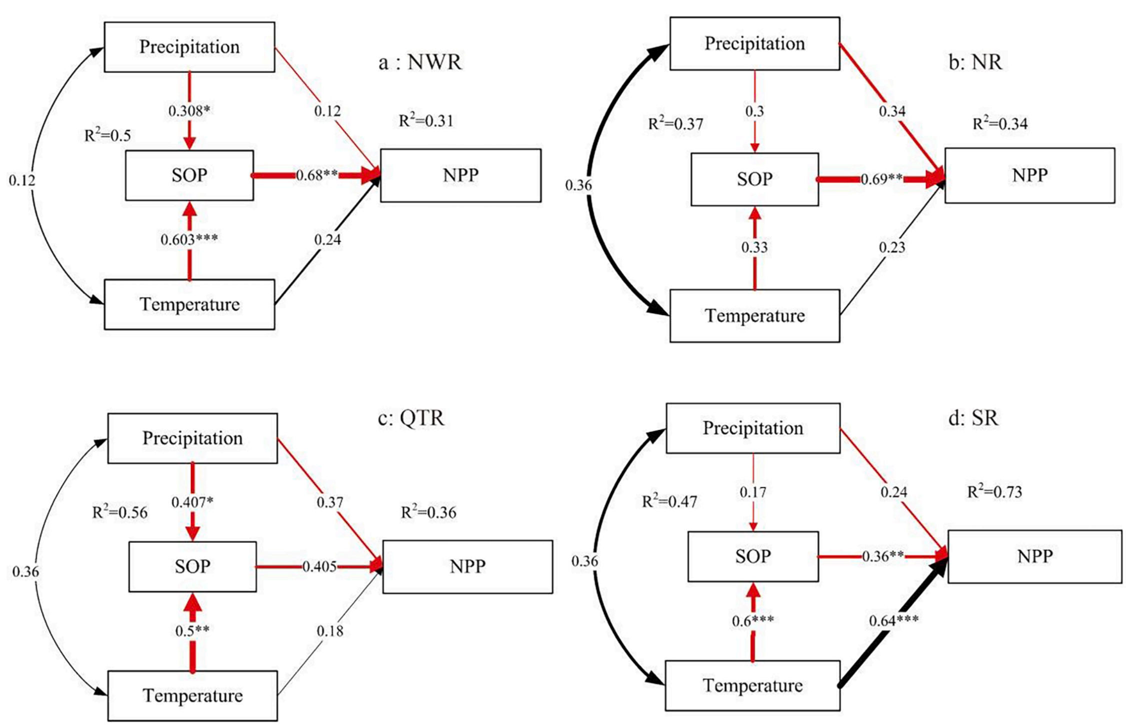

Fig. 5. Structural equation modeling results between temperature precipitation, SOP and NPP for the four regions. In Figure 7, boxes indicate observed variables; one-way arrows indicate effect relationships between two variables, with the variable indicated by the arrow being influenced by another variable. Double-headed arrows indicate associations between variables. The numbers near the single or double-headed arrows are normalization coefficients, and the black lines (macros) of the arrows indicate positive (negative) relationships, respectively; the thicker the line, the stronger the relationship. **** is the significance level of 0.01, 0.05 and 0.1, respectively, and R^2 is the magnitude of the variance being explained.

4.2. Climate controls on the SOP in China

We found that there was a negative correlation between the SOP and the mean pre-season temperature in most quadrats (76%) of the study area, which demonstrates that a warm spring does advance the SOP in the southwest. This is consistent with previous findings that vegetation regrowth advances with increasing temperature based on vegetation indices such as the NDVI and EVI (Cong et al., 2013a; Ge et al., 2015; Jeong et al., 2011; Piao et al., 2006; Shen et al., 2022; Zhou et al., 2020). The correlation between the SOP and the pre-season temperature was more significant than that between the SOP and the pre-season precipitation, indicating that temperature remains the main determinant of the SOP in China, which is also consistent with previous results obtained in the northern temperate zone (Piao et al., 2006). We observed that there was gradual weakening of the bias correlation coefficient between the temperature and SOP along the weakening precipitation gradient (from east to west) and a shift in the determinant from temperature to precipitation. It has previously been shown that vegetation growth requires more heat supplementation when pre-season precipitation is high (Fu et al., 2014; Gao et al., 2022), that under relatively wet conditions (i.e., areas with higher average pre-season precipitation), the SOP has more access to water accessible and vegetation growth is not limited by water scarcity (Chen et al., 2014; Gao et al., 2022; Zhang et al., 2005), and the SOPs are more sensitive to temperature due to the demand for heat. In addition, temperature increases caused by anthropogenic land use (e.g., spring ploughing and grazing, etc.) also contribute to the early SOP (Li et al., 2019; Morisette et al., 2009). Since the 1980s, temperatures in crop-growing areas have increased significantly at an average rate of 0.06 °C/a, which is one reason for the early planting in these areas (Piao et al., 2006). There are also a number of quadrates in which temperature is positively correlated with the SOP, possibly because a certain amount of cumulative low temperature is required to break the natural dormancy of vegetation prior to the onset of spring phenological events, and the associated winter warming results in insufficient low temperatures (Fu et al., 2015; Piao et al., 2019).

In relative terms, the bias correlation coefficient between precipitation and the SOP gradually increases along the weakening precipitation gradient, with the determinant shifting from temperature in the east to precipitation in the west, indicating the increasing importance of precipitation as the pre-season accumulated precipitation decreases. In areas with low average pre-season precipitation, the soil moisture may not reach optimal moisture conditions in spring, when the SOP is determined by precipitation rather than temperature (Shen et al., 2015). The higher evapotranspiration in these areas reduces water availability and may delay the SOP under future warming conditions (Yu et al., 2003).

As a result, the relative importance of precipitation and temperature changes under different rainfall conditions. We speculate that future warming may further advance the SOP in areas with higher average pre-season precipitation; while in areas with lower average pre-season precipitation, limited by increased moisture availability and evapotranspiration, warming will have less impact on the SOP in China or even delay it. Future warming and drying of the climate will further expand areas of limited water resources and the control of precipitation on the SOP in China will increase (Zhang et al., 2020).

4.3. Impacts of SOP advancement and climate change on NPP

Temperature and precipitation directly affect the NPP. In general, both temperature and precipitation led to an increase in the NPP from 2001 to 2020. Compared with other regions, the SR region had the highest direct positive influence on the temperature. This may be because the Yunnan-Guizhou Plateau and other parts of this region are characterized by higher altitudes and abundant precipitation, but the sunshine duration and solar radiation are lower, thus limiting the growth of vegetation (Bai et al., 2023). Therefore, the rising temperature is conducive to the photosynthesis of vegetation, thus promoting vegetation growth (Yu et al., 2023). Regarding precipitation, the increase in precipitation improves the supply of soil water and increases the photosynthetic rate (Sun and Du, 2017). Therefore, the precipitation in these four regions of China has a direct positive impact on the NPP, and the precipitation in the QTR has the greatest direct impact. This may be due to the fact that the forests on the Qinghai-Tibet Plateau are mostly distributed in the east and southeast, where the temperature is higher. The amount of precipitation directly affects the growth of vegetation (Zhang et al., 2014b). A large part of the grassland in central China is distributed in the Gobi desert and saline-alkali land, the long-term water shortages in these areas increases the importance of precipitation (Bai et al., 2021; Ma et al., 2022b), and the sensitivity of the grassland to precipitation is also higher (Yu et al.,2023). These factors combine to increase the direct impact of precipitation.

Structural equation modeling shows that the NPP in all four regions is indirectly influenced by climate change. Climate change affects the vegetation productivity in two ways, either by directly affecting vegetation growth and photosynthesis, and by changing the phenology (Fang et al., 2003; Piao et al., 2007; Piao et al., 2017; Wan et al., 2005). The SIF has a greater potential as a direct proxy for photosynthesis than indices such as the NDVI and EVI for monitoring phenology and productivity in evergreen forests (Zhang et al., 2022b). The NPP has increased since the 1980s (Nemani et al., 2003),

The increase in the NPP may be mainly be the result of a longer growing season, particularly an increase in vegetation activity in early spring (Fang et al., 2003; Gu et al., 2022; Randerson et al., 1999). This is probably because the solar radiation and moisture conditions are most favorable for vegetation productivity in spring (Smith et al., 2004) when the photosynthetic carbon uptake is greater than respiratory carbon release (Keeling et al., 1996), and vegetation can fix more carbon thereby increasing the terrestrial ecosystem carbon sink. In addition, despite the increase in temperature, soil temperatures are still relatively low and do not significantly increase soil respiration (Randerson et al., 1999); however, this progression may shift under future warming, and earlier advancement of the SOP may exacerbate soil water loss causing summer drought stress and thus reducing productivity (Fu, 2022b; Piao, 2008; Zhang et al., 2020). Additionally, recent studies have shown that there is a significant decrease in the effect of increasing temperature on spring carbon uptake (Piao, 2017a; Wang, 2018), further suggesting the importance of future precipitation in related research.

4.4. Limitations and prospects

Based on remote sensing images, in this study, the response of the SOP to climate change and its impact on the NPP over the past 20 years were investigated. Although important basic results were attained, this study also has some limitations.

The SOP and NPP are affected by multiple climatic factors, and in this study, only temperature and precipitation were considered. Although these factors are considered to be the main driving factors (Korner and Basler, 2010; Liu et al., 2016; Menzel et al., 2006; Tao et al., 2017), other climatic factors should also be considered in future studies, including the photoperiod (Flynn and Wolkovich, 2018), nutrient (Fu et al., 2019), air humidity (Sparks and Menzel, 2002), and phenological interaction (Buermann et al., 2013). In addition, the impacts of human activities on climate change and the NPP are increasing (Ge et al., 2021). Although we used land use data to exclude arable land in our study, it is still not possible to completely exclude the impact of human activities on climate change and the SOP. Therefore, the relationships between human activities and the SOP and NPP need to be further investigated in the future.

Conclusions

In this study, we assessed the spatial and temporal patterns affecting

SOP in China and its main controlling climate factors, revealing the interrelationship between SOP and NPP. Our conclusions are as follows:

(1) In the last 20 years, the average SOP in China was on the 123rd day of the year, and the SOP has advanced at an average rate of 4.3 d $(10\ a)^{-1}$, with SOP advancing more rapidly in highland and high-altitude areas;
(2) 64% of SOP in China are controlled by temperature; 36% of SOP in China are controlled by precipitation;
(3) As the precipitation gradient decreases the relative importance of temperature and precipitation reverses, with SOP dominated by temperature control for pre-season precipitation ≧300 mm and precipitation control for pre-season precipitation ≦300 mm;
(4) Future warming and drying of the climate will further expand the area of limited water resources, making precipitation increasingly important for the control of the SW SOP;
(5) Climate change indirectly increases vegetation NPP through earlier SOP.

Our results highlight the importance of future precipitation for SOP and find that climate change indirectly increases NPP by advancing SOP. Our study has important implications for research on the carbon cycle in terrestrial ecosystems.

Data availability statement

The fundamental data used in our study is available to the public, and their websites are provided in the "2. Materials and methods" section other data are available from the corresponding author upon reasonable request.

CRediT authorship contribution statement

Yingying Xue: Conceptualization, Formal analysis, Writing – original draft. **Xiaoyong Bai:** Conceptualization, Supervision, Resources. **Cuiwei Zhao:** . **Qiu Tan:** Validation, Project administration. **Yangbing Li:** Validation, Project administration. **Guangjie Luo:** Validation, Project administration. **Luhua Wu:** Validation, Formal analysis. **Fei Chen:** Validation, Formal analysis. **Chaojun Li:** Validation, Formal analysis. **Chen Ran:** Validation, Formal analysis. **Sirui Zhang:** Validation, Formal analysis. **Min Liu:** Validation, Formal analysis. **Suhua Gong:** Data curation, Writing – review & editing. **Lian Xiong:** Data curation, Writing – review & editing. **Fengjiao Song:** Data curation, Writing – review & editing. **Chaochao Du:** Data curation, Writing – review & editing. **Biqin Xiao:** Visualization. **Zilin Li:** Visualization. **Mingkang Long:** Visualization.

Declaration of Competing Interest

The authors declare that they have no known competing financial interests or personal relationships that could have appeared to influence the work reported in this article.

Acknowledgments

This research work was supported by Joint Foundation of Jo National Natural Science Foundation (No. U22A20619), National Nature Science Foundations of China (No. 42077455), Western Light Cross-team Program of Chinese Academy of Sciences (No. xbzg-zdsys-202101), Strategic Priority Research Program of the Chinese Academy of Sciences (No. XDB40000000 & No. XDA23060100), Guizhou Provincial Science and Technology Projects (No. Qiankehe Support [2023] General 219 & [2023] Key 010), High-level Innovative Talents in Guizhou Province (No. GCC[2022]015-1 & No. 2016-5648), Guizhou Provincial Science and Technology Subsidies (No. GZ2019SIG & No. GZ2020SIG).We thank LetPub (www.letpub.com) for its linguistic assistance during the preparation of this manuscript.

References

Aono, Y., Kazui, K., 2008. Phenological data series of cherry tree flowering in Kyoto, Japan, and its application to reconstruction of springtime temperatures since the 9th century. Int. J. Climatol. 28 (7), 905–914.

Aronson, E.L., McNulty, S.G., 2009. Appropriate experimental ecosystem warming methods by ecosystem, objective, and practicality. Agric. For. Meteorol. 149 (11), 1791–1799.

Bai, X.H., Zhao, W.W., Wang, J., Ferreira, C.S.S., 2021. Precipitation drives the floristic composition and diversity of temperate grasslands in China. Glob. Ecol. Conserv. 32.

Bai, X., et al., 2023. A carbon-neutrality-capactiy index for evaluating carbon sink contributions. Environ. Sci. Ecotechnol. 15.

Buermann, W., Bikash, P.R., Jung, M., Burn, D.H., Reichstein, M., 2013. Earlier springs decrease peak summer productivity in North American boreal forests. Environ. Res. Lett. 8 (2).

Buyantuyev, A., Wu, J.G., 2012. Urbanization diversifies land surface phenology in arid environments: interactions among vegetation, climatic variation, and land use pattern in the Phoenix metropolitan region, USA. Landsc. Urban Plan. 105 (1–2), 149–159.

Chen, A., et al., 2021. Moisture availability mediates the relationship between terrestrial gross primary production and solar-induced chlorophyll fluorescence: insights from global-scale variations. Glob. Chang. Biol. 27 (6), 1144–1156.

Chen, A., Meng, F., Mao, J., Ricciuto, D., 2022a. Photosynthesis phenology, as defined by solar-induced chlorophyll fluorescence, is overestimated by vegetation indices in the extratropical Northern Hemisphere. Agric. For. Meteorol. 323.

Chen, A.P., Meng, F.D., Mao, J.F., Ricciuto, D., 2022b. Photosynthesis phenology, as defined by solar-induced chlorophyll fluorescence, is overestimated by vegetation indices in the extratropical Northern Hemisphere. Agric. For. Meteorol. 323.

Chen, L., et al., 2018. Spring phenology at different altitudes is becoming more uniform under global warming in Europe. Glob. Chang. Biol. 24 (9), 3969–3975.

Chen, X., An, S., Inouye, D.W., Schwartz, M.D., 2015. Temperature and snowfall trigger alpine vegetation green-up on the world's roof. Glob. Chang. Biol. 21 (10), 3635–3646.

Chen, X., Li, J., Xu, L., Liu, L., Ding, D., 2014. Modeling greenup date of dominant grass species in the Inner Mongolian Grassland using air temperature and precipitation data. Int. J. Biometeorol. 58 (4), 463–471.

Cong, N., et al., 2013a. Changes in satellite-derived spring vegetation green-up date and its linkage to climate in China from 1982 to 2010: a multimethod analysis. Glob. Chang. Biol. 19 (3), 881–891.

Cong, N., et al., 2013b. Changes in satellite-derived spring vegetation green-up date and its linkage to climate in China from 1982 to 2010: a multimethod analysis. Glob. Chang. Biol. 19 (3), 881–891.

Dai, J.H., et al., 2021. Divergent changes of the elevational synchronicity in vegetation spring phenology in North China from 2001 to 2017 in connection with variations in chilling. Int. J. Climatol. 41 (13), 6109–6121.

Fang, J.Y., et al., 2003. Increasing net primary production in China from 1982 to 1999. Front. Ecol. Environ. 1 (6), 293–297.

Flynn, D.F.B., Wolkovich, E.M., 2018. Temperature and photoperiod drive spring phenology across all species in a temperate forest community. New Phytol. 219 (4), 1353–1362.

Forkel, M., et al., 2016. Enhanced seasonal CO_2 exchange caused by amplified plant productivity in northern ecosystems. Science 351 (6274), 696–699.

Fu, Y.S., et al., 2022a. Vegetation phenology response to climate change in China. J. Beijing Normal Univ. (Nat. Sci.) 58 (03), 424–433.

Fu, Y.H., et al., 2022b. Soil moisture regulates warming responses of autumn photosynthetic transition dates in subtropical forests. Glob. Chang. Biol. 28 (16), 4935–4946.

Fu, Y.H., et al., 2014. Unexpected role of winter precipitation in determining heat requirement for spring vegetation green-up at northern middle and high latitudes. Glob. Chang. Biol. 20 (12), 3743–3755.

Fu, Y.H., et al., 2015. Declining global warming effects on the phenology of spring leaf unfolding. Nature 526 (7571), 104.

Fu, Y.S.H., et al., 2019. Nutrient availability alters the correlation between spring leaf-out and autumn leaf senescence dates. Tree Physiol. 39 (8), 1277–1284.

Gao, S., et al., 2022. An earlier start of the thermal growing season enhances tree growth in cold humid areas but not in dry areas. Nat. Ecol. Evol. 6 (4), 397.

Ge, Q., Wang, H., Rutishauser, T., Dai, J., 2015. Phenological response to climate change in China: a meta-analysis. Glob. Chang. Biol. 21 (1), 265–274.

Ge, W.Y., Deng, L.Q., Wang, F., Han, J.Q., 2021. Quantifying the contributions of human activities and climate change to vegetation net primary productivity dynamics in China from 2001 to 2016. Sci. Total Environ. 773.

Gentine, P., Alemohammad, S.H., 2018. Reconstructed solar-induced fluorescence: a machine learning vegetation product based on MODIS surface reflectance to reproduce GOME-2 solar-induced fluorescence. Geophys. Res. Lett. 45 (7), 3136–3146.

Gill, A.L., et al., 2015. Changes in autumn senescence in northern hemisphere deciduous trees: a meta-analysis of autumn phenology studies. Ann. Bot. 116 (6), 875–888.

Gu, H., et al., 2022. Warming-induced increase in carbon uptake is linked to earlier spring phenology in temperate and boreal forests (vol 13, 3698, 2022). Nat. Commun. 13 (1).

Hao, J., et al., 2020. Quantifying the relative contribution of natural and human factors to vegetation coverage variation in coastal wetlands in China. Catena 188.

Hu, J., Moore, D.J.P., Burns, S.P., Monson, R.K., 2010. Longer growing seasons lead to less carbon sequestration by a subalpine forest. Glob. Chang. Biol. 16 (2), 771–783.
Hu, Z.M., et al., 2022. Decoupling of greenness and gross primary productivity as aridity decreases. Rem. Sens. Environ. 279.
Hunter, A.F., Lechowicz, M.J., 1992. Predicting the timing of budburst in temperate trees. J. Appl. Ecol. 29 (3), 597–604.
Jeong, S.-J., Ho, C.-H., Gim, H.-J., Brown, M.E., 2011. Phenology shifts at start vs. end of growing season in temperate vegetation over the Northern Hemisphere for the period 1982-2008. Glob. Chang. Biol. 17 (7), 2385–2399.
Jeong, S.-J., et al., 2017. Application of satellite solar-induced chlorophyll fluorescence to understanding large-scale variations in vegetation phenology and function over northern high latitude forests. Rem. Sens. Environ. 190, 178–187.
Jiao, F.S., Liu, H.Y., Xu, X.J., Gong, H.B., Lin, Z.S., 2020. Trend evolution of vegetation phenology in china during the period of 1981-2016. Rem. Sens. (Basel) 12 (3).
Joiner, J., et al., 2014. The seasonal cycle of satellite chlorophyll fluorescence observations and its relationship to vegetation phenology and ecosystem atmosphere carbon exchange. Rem. Sens. Environ 152, 375–391.
Keeling, C.D., Chin, J.F.S., Whorf, T.P., 1996. Increased activity of northern vegetation inferred from atmospheric CO2 measurements. Nature 382 (6587), 146–149.
Keenan, T.F., et al., 2014. Net carbon uptake has increased through warming-induced changes in temperate forest phenology. Nat. Clim. Chang. 4 (7), 598–604.
Kendall, M.G., 1938. A new measure of rank correlation. Biometrika 30, 81–93.
Korner, C., Basler, D., 2010. Phenology under global warming. Science 327 (5972), 1461–1462.
Li, G., Jiang, C., Cheng, T., Bai, J., 2019. Grazing alters the phenology of alpine steppe by changing the surface physical environment on the northeast Qinghai-Tibet Plateau. China. J. Environ. Manag. 248.
Li, J.H., et al., 2023a. Important role of precipitation in controlling a more uniform spring phenology in the Qinba Mountains. China. Front. Plant Sci. 14.
Li, L., Zha, Y., 2019. Satellite-based spatiotemporal trends of canopy urban heat islands and associated drivers in China's 32 major cities. Rem. Sens. (Basel) 11 (1).
Li, X., et al., 2021a. Increasing importance of precipitation in spring phenology with decreasing latitudes in subtropical forest area in China. Agric. For. Meteorol. 304.
Li, X., et al., 2018a. Solar-induced chlorophyll fluorescence is strongly correlated with terrestrial photosynthesis for a wide variety of biomes: first global analysis based on OCO-2 and flux tower observations. Glob. Chang. Biol. 24 (9), 3990–4008.
Li, X.X., et al., 2021b. Increasing importance of precipitation in spring phenology with decreasing latitudes in subtropical forest area in China. Agric. For. Meteorol. 304.
Li, Y., et al., 2022. Effects of land use and land cover change on soil organic carbon storage in the Hexi regions. Northwest China. J. Environ. Manag. 312.
Li, Y., et al., 2023b. The role of land use change in affecting ecosystem services and the ecological security pattern of the Hexi Regions, Northwest China. Sci. Total Environ. 855.
Li, Y., et al., 2018b. Divergent hydrological response to large-scale afforestation and vegetation greening in China. Sci. Adv. 4 (5).
Lian, X., et al., 2020. Summer soil drying exacerbated by earlier spring greening of northern vegetation. Sci. Adv. 6 (1).
Liu, Q., et al., 2016. Temperature, precipitation, and insolation effects on autumn vegetation phenology in temperate China. Glob. Chang. Biol. 22 (2), 644–655.
Luo, Z.H., Yu, S.X., 2017. Spatiotemporal variability of land surface phenology in China from 2001 to 2014. Rem. Sens. (Basel) 9 (1).
Ma, P.F., Zhao, J.X., Zhang, H.Z., Zhang, L., Luo, T.X., 2023. Increased precipitation leads to earlier green-up and later senescence in Tibetan alpine grassland regardless of warming. Sci. Total Environ. 871.
Ma, R., et al., 2022a. Variation of vegetation autumn phenology and its climatic drivers in temperate grasslands of China. Int. J. Appl. Earth Obs. Geoinf. 114.
Ma, R., et al., 2022b. Spatiotemporal change of net primary productivity and its response to climate change in temperate grasslands of China. Front. Plant Sci. 13.
Ma, T., Zhou, C.G., 2012. Climate-associated changes in spring plant phenology in China. Int. J. Biometeorol. 56 (2), 269–275.
Meng, F., Huang, L., Chen, A., Zhang, Y., Piao, S., 2021. Spring and autumn phenology across the Tibetan Plateau inferred from normalized difference vegetation index and solar-induced chlorophyll fluorescence. Big Earth Data 5 (22), 1–19.
Menzel, A., et al., 2006. European phenological response to climate change matches the warming pattern. Glob. Chang. Biol. 12 (10), 1969–1976.
Morisette, J.T., et al., 2009. Tracking the rhythm of the seasons in the face of global change: phenological research in the 21st century. Front. Ecol. Environ. 7 (5), 253–260.
Murray, M.B., Cannell, M.G.R., Smith, R.I., 1989. Date of budburst of 15 tree species in Britain following climatic warming. J. Appl. Ecol. 26 (2), 693–700.
Nemani, R.R., et al., 2003. Climate-driven increases in global terrestrial net primary production from 1982 to 1999. Science 300 (5625), 1560–1563.
Parmesan, C., 2007. Influences of species, latitudes and methodologies on estimates of phenological response to global warming. Glob. Chang. Biol. 13 (9), 1860–1872.
Paulina, K., Torbern, T., Rasmus, F., 2017. Evaluation of the plant phenology index (PPI), NDVI and EVI for start-of-season trend analysis of the Northern Hemisphere Boreal Zone. Rem. Sens. (Basel) 9 (5), 485.
Peng, K., Jiang, W., Ling, Z., Hou, P., Deng, Y., 2021. Evaluating the potential impacts of land use changes on ecosystem service value under multiple scenarios in support of SDG reporting: a case study of the Wuhan urban agglomeration. J. Clean. Prod. 307.
Piao, S., et al., 2008. Net carbon dioxide losses of northern ecosystems in response to autumn warming. Nature 451 (7174), 49.
Piao, S., Friedlingstein, P., Ciais, P., Viovy, N., Demarty, J., 2007. Growing season extension and its impact on terrestrial carbon cycle in the Northern Hemisphere over the past 2 decades. Glob. Biogeochem. Cycles 21 (3).
Piao, S., et al., 2019. Plant phenology and global climate change: current progresses and challenges. Glob. Chang. Biol. 25 (6), 1922–1940.
Piao, S., et al., 2017a. Weakening temperature control on the interannual variations of spring carbon uptake across northern lands. Nat. Clim. Chang. 7 (5), 359.
Piao, S.L., Fang, J.Y., Zhou, L.M., Ciais, P., Zhu, B., 2006. Variations in satellite-derived phenology in China's temperate vegetation. Glob. Chang. Biol. 12 (4), 672–685.
Piao, S.L., et al., 2017b. Weakening temperature control on the interannual variations of spring carbon uptake across northern lands. Nat. Clim. Chang. 7 (5), 359.
Qiu, T., Song, C.H., Zhang, Y.L., Liu, H.S., Vose, J.M., 2020. Urbanization and climate change jointly shift land surface phenology in the northern mid-latitude large cities. Rem. Sens. Environ. 236.
Randerson, J.T., Field, C.B., Fung, I.Y., Tans, P.P., 1999. Increases in early season ecosystem uptake explain recent changes in the seasonal cycle of atmospheric CO2 at high northern latitudes. Geophys. Res. Lett. 26 (17), 2765–2768.
Ran, C., et al., 2023. Threat of soil formation rate to health of karst ecosystem. Sci. Total Environ. 887.
Ren, S.L., Chen, X.Q., Pan, C.C., 2022. Temperature-precipitation background affects spatial heterogeneity of spring phenology responses to climate change in northern grasslands (30 degrees N-55 degrees N). Agric. For. Meteorol. 315.
Ren, S.L., Peichl, M., 2021. Enhanced spatiotemporal heterogeneity and the climatic and biotic controls of autumn phenology in northern grasslands. Sci. Total Environ. 788.
Richardson, A.D., et al., 2013. Climate change, phenology, and phenological control of vegetation feedbacks to the climate system. Agric. For. Meteorol. 169, 156–173.
Schwartz, M.D., 2003. Phenology: an integrative environmental science - introduction. Phenol.: Integr. Environ. Sci. 39, 3–7.
Shen, M., Piao, S., Cong, N., Zhang, G., Janssens, I.A., 2015. Precipitation impacts on vegetation spring phenology on the Tibetan Plateau. Glob. Chang. Biol. 21 (10), 3647–3656.
Shen, M., Tang, Y., Chen, J., Zhu, X., Zheng, Y., 2011a. Influences of temperature and precipitation before the growing season on spring phenology in grasslands of the central and eastern Qinghai-Tibetan Plateau. Agric. For. Meteorol. 151 (12), 1711–1722.
Shen, M., et al., 2022. Plant phenology changes and drivers on the Qinghai-Tibetan Plateau. Nat. Rev. Earth Environ.
Shen, M.G., Piao, S.L., Cong, N., Zhang, G.X., Janssens, I.A., 2015b. Precipitation impacts on vegetation spring phenology on the Tibetan Plateau. Glob. Chang. Biol. 21 (10), 3647–3656.
Shen, M.G., Tang, Y.H., Chen, J., Zhu, X.L., Zheng, Y.H., 2011b. Influences of temperature and precipitation before the growing season on spring phenology in grasslands of the central and eastern Qinghai-Tibetan Plateau. Agric. For. Meteorol. 151 (12), 1711–1722.
Shen, X.J., et al., 2018. Asymmetric effects of daytime and nighttime warming on spring phenology in the temperate grasslands of China. Agric. For. Meteorol. 259, 240–249.
Smith, L.C., et al., 2004. Siberian peatlands a net carbon sink and global methane source since the early Holocene. Science 303 (5656), 353–356.
Smith, W.K., et al., 2018. Chlorophyll fluorescence better captures seasonal and interannual gross primary productivity dynamics across dryland ecosystems of Southwestern North America. Geophys. Res. Lett. 45 (2), 748–757.
Sparks, T.H., Menzel, A., 2002. Observed changes in seasons: an overview. Int. J. Climatol. 22 (14), 1715–1725.
Steltzer, H., Post, E., 2009. Seasons and life cycles. Science 324 (5929), 886–887.
Stone, B.M., 2021. The ethical use of fit indices in structural equation modeling: recommendations for psychologists. Front. Psychol. 12, 83226. -83226.
Sun, J., Du, W.P., 2017. Effects of precipitation and temperature on net primary productivity and precipitation use efficiency across China's grasslands. GIsci Rem. Sens. 54 (6), 881–897.
Tan, X.Y., Jia, Y.W., Yang, D.W., Niu, C.W., Hao, C.F., 2023. Turning points in the impact of earlier green-up on evapotranspiration and gross primary productivity in a semi-arid grassland watershed. J. Hydrol. (Amst) 616.
Tao, Z.X., Wang, H.J., Liu, Y.C., Xu, Y.J., Dai, J.H., 2017. Phenological response of different vegetation types to temperature and precipitation variations in northern China during 1982-2012. Int. J. Rem. Sens. 38 (11), 3236–3252.
Wan, S.Q., Hui, D.F., Wallace, L., Luo, Y.Q., 2005. Direct and indirect effects of experimental warming on ecosystem carbon processes in a tallgrass prairie. Glob. Biogeochem. Cycles 19 (2).
Wang, C., Cao, R., Chen, J., Rao, Y., Tang, Y., 2015. Temperature sensitivity of spring vegetation phenology correlates to within-spring warming speed over the Northern Hemisphere. Ecol. Indic. 50, 62–68.
Wang, C., et al., 2022a. Comparison of vegetation phenology derived from solar-induced chlorophyll fluorescence and enhanced vegetation index, and their relationship with climatic limitations. Rem. Sens. (Basel) 14 (13).
Wang, C., et al., 2022b. Comparison of vegetation phenology derived from solar-induced chlorophyll fluorescence and enhanced vegetation index, and their relationship with climatic limitations. Rem. Sens. (Basel) 14 (13).
Wang, H.J., Dai, J.H., Zheng, J.Y., Ge, Q.S., 2015b. Temperature sensitivity of plant phenology in temperate and subtropical regions of China from 1850 to 2009. Int. J. Climatol. 35 (6), 913–922.
Wang, T., et al., 2018. Emerging negative impact of warming on summer carbon uptake in northern ecosystems. Nat. Commun. 9.
Wang, T., et al., 2014a. The influence of local spring temperature variance on temperature sensitivity of spring phenology. Glob. Chang. Biol. 20 (5), 1473–1480.
Wang, T., et al., 2014b. The influence of local spring temperature variance on temperature sensitivity of spring phenology. Glob. Chang. Biol. 20 (5), 1473–1480.
Wang, X., Sun, Z.Q., Lu, S., Zhang, Z.X., 2022c. Comparison of phenology estimated from monthly vegetation indices and solar-induced chlorophyll fluorescence in China. Front. Earth Sci. 10.

Weterings, R., Umponstira, C., Buckley, H.L., 2018. Landscape variation influences trophic cascades in dengue vector food webs. Sci. Adv. 4 (2).
Xiao, B., et al., 2023. Responses of carbon and water use efficiencies to climate and land use changes in China's karst areas. J. Hydrol. (Amst) 617.
Yang, J., Zhang, X.C., Luo, Z.H., Yu, X.J., 2017. Nonlinear variations of net primary productivity and its relationship with climate and vegetation phenology. China. For. 8 (10).
Yao, Y., et al., 2018. Spatiotemporal pattern of gross primary productivity and its covariation with climate in China over the last thirty years. Glob. Chang. Biol. 24 (1), 184–196.
Ye, Q.J., Li, Z.W., Duan, L.X., Xu, X.L., 2022. Decoupling the influence of vegetation and climate on intra-annual variability in runoff in karst watersheds. Sci. Total Environ. 824.
Yu, F.F., Price, K.P., Ellis, J., Shi, P.J., 2003. Response of seasonal vegetation development to climatic variations in eastern central Asia. Rem. Sens. Environ. 87 (1), 42–54.
Yu, Z., et al., 2022. Forest expansion dominates China's land carbon sink since 1980. Nat. Commun. 13 (1).
Yu, H.Y., et al., 2023. Analysis of spatio-temporal variation characteristics and influencing factors of net primary productivity in terrestrial ecosystems of China. Acta Ecol. Sin. 43 (03), 1219–1233.
Zeng, L., Wardlow, B.D., Xiang, D., Hu, S., Li, D., 2020a. A review of vegetation phenological metrics extraction using time-series, multispectral satellite data. Rem. Sens. Environ. 237.
Zeng, L.L., Wardlow, B.D., Xiang, D.X., Hu, S., Li, D.R., 2020b. A review of vegetation phenological metrics extraction using time-series, multispectral satellite data. Rem. Sens. Environ. 237.
Zhang, G., Zhang, Y., Dong, J., Xiao, X., 2013. Green-up dates in the Tibetan Plateau have continuously advanced from 1982 to 2011. Proc. Natl. Acad. Sci. U.S.A. 110 (11), 4309–4314.
Zhang, J., Chen, S.Z., Wu, Z.F., Fu, Y.H., 2022a. Review of vegetation phenology trends in China in a changing climate. Prog. Phys. Geogr. -Earth Environ. 46 (6), 829–845.
Zhang, J., et al., 2022b. NIRv and SIF better estimate phenology than NDVI and EVI: effects of spring and autumn phenology on ecosystem production of planted forests. Agric. For. Meteorol. 315.
Zhang, J.R., et al., 2022c. NIRv and SIF better estimate phenology than NDVI and EVI: effects of spring and autumn phenology on ecosystem production of planted forests. Agric. For. Meteorol. 315.
Zhang, X.Y., Friedl, M.A., Schaaf, C.B., Strahler, A.H., Liu, Z., 2005. Monitoring the response of vegetation phenology to precipitation in Africa by coupling MODIS and TRMM instruments. J. Geophys. Res.-Atmos. 110 (D12).
Zhang, Y., et al., 2014a. Estimation of vegetation photosynthetic capacity from space-based measurements of chlorophyll fluorescence for terrestrial biosphere models. Glob. Chang Biol. 20 (12), 3727–3742.
Zhang, Y., Joiner, J., Alemohammad, S.H., Zhou, S., Gentine, P., 2018. A global spatially contiguous solar-induced fluorescence (CSIF) dataset using neural networks. Biogeosciences 15 (19), 5779–5800.
Zhang, Y., Parazoo, N.C., Williams, A.P., Zhou, S., Gentine, P., 2020. Large and projected strengthening moisture limitation on end-of-season photosynthesis. Proc. Natl. Acad. Sci. U.S.A. 117 (17), 9216–9222.
Zhang, Y.L., et al., 2014b. Spatial and temporal variability in the net primary production of alpine grassland on the Tibetan Plateau since 1982. J. Geog. Sci. 24 (2), 269–287.
Zhou, D.C., Zhao, S.Q., Zhang, L.X., Liu, S.G., 2016. Remotely sensed assessment of urbanization effects on vegetation phenology in China's 32 major cities. Rem. Sens. Environ. 176, 272–281.
Zhou, X., et al., 2020. Legacy effect of spring phenology on vegetation growth in temperate China. Agric. For. Meteorol. 281.